

Modelling of creep curves of Ni₃Ge single crystals

V A Starenchenko¹, S V Starenchenko¹, O D Pantyukhova¹ and Yu V Solov'eva¹

¹Tomsk State University of Architecture and Building, Tomsk, 634003, Russia

E-mail: sve-starenchenko@yandex.ru

Abstract. In this paper the creep model of alloys with $L1_2$ superstructure is presented. The creep model is based on the idea of the mechanisms superposition connected with the different elementary deformation processes. Some of them are incident to the ordered structure $L1_2$ (anomalous mechanisms), others are typical to pure metals with the fcc structure (normal mechanisms): the accumulation of thermal APBs by means of the intersection of moving dislocations; the formation of APB tubes; the multiplication of superdislocations; the movement of single dislocations; the accumulation of point defects, such as vacancies and interstitial atoms; the accumulation APBs at the climb of edge dislocations. This model takes into account the experimental facts of the wetting antiphase boundaries and emergence of the disordered phase within the ordered phase. The calculations of the creep curves are performed under different conditions. This model describes different kinds of the creep curves and demonstrates the important meaning of the deformation superlocalisation leading to the inverse creep. The experimental and theoretical results coincide rather well.

1. Introduction

The creep of the Ni₃Ge alloy with $L1_2$ superstructure possesses a number of peculiarities that differ it from the creep of pure metals with fcc structure. Low rate of creep under moderate temperature, anomalous creep dependence under certain temperature intervals and the presence of creep with constant rate in the high temperature areas refer to them [1-6].

The temperature influence on dislocations movement in the alloy can explain these peculiarities. The influence has a double nature. On the one hand the temperature increase causes the superdislocations mobility rise. On the other hand a part of superdislocations are happened to be blocked into stable configurations, being higher with the temperature increase [7]. This paper is dedicated to the model where the peculiarities of superdislocations movement and the influence of temperature changes on it are considered. The calculations are performed and the possibility of some peculiarities of the Ni₃Ge alloy creep to be described in the suggested model is shown.

2. Modelling

The papers [8-10] give the formulation of the mathematical model of single crystal alloys creep with $L1_2$ superstructure, the concept of strengthening and rest being the basis of it [11-12].



Due to the concept mathematical formulation of the model of single crystal alloys creep with superstructure $L1_2$ oriented for multiplication of slipping is the following [8, 9] (1).

$$\left. \begin{aligned} \frac{da}{dt} &= \rho_s^* b v_D (\xi \rho)^{-1/2} \left(\exp \left[-\frac{U - \tau_s b^2 l_{cp}}{kT} \right] + \exp \left[-\frac{U + \tau_s b^2 l_{cp}}{kT} \right] \right), \\ \frac{d\rho}{dt} &= \dot{a} \left(C_1 \frac{(\alpha G b)^2 \rho}{\tau_f^0 + \tau_f + \alpha G b \rho^{1/2}} + \frac{C_2 e^{-U_1/kT} + C_3 e^{-U_2/kT}}{G b \rho^{1/2}} \right) - \\ &\quad - \min(r_a, [\theta \rho]^{-1/2}) \frac{a_l^3 D_0}{\chi k T b} \left(\exp \left[\frac{-E_i}{kT} \right] \cdot C_i + \exp \left[\frac{-E_v}{kT} \right] \cdot C_v \right) \tau \rho^2 \theta^2, \\ \frac{dC_i}{dt} &= \dot{a} \frac{1}{\kappa(\zeta)} p_j \xi B \frac{\tau}{G} - \frac{a_l^3 D_0}{\chi k T} \exp \left[\frac{-E_i}{kT} \right] C_i \tau \rho \theta - \mu_r D_0 \exp \left[\frac{-E_i}{kT} \right] C_i C_v, \\ \frac{dC_v}{dt} &= \dot{a} \frac{1}{\kappa(\zeta)} p_j \xi B \frac{\tau}{G} - \frac{a_l^3 D_0}{\chi k T} \exp \left[\frac{-E_v}{kT} \right] C_v \tau \rho \theta - \mu_r D_0 \exp \left[\frac{-E_i}{kT} \right] C_i C_v, \\ \tau &= const \quad (P = const). \end{aligned} \right\} \quad (1)$$

The materials ductile deformation is known to be realized by the dislocation movement thus forming shear zones. In the model for the alloys with $L1_2$ superstructure all dislocations are divided into peripheral and intrazone dislocations. The former are retarded shear-forming dislocations at the periphery of the shear zone, the latter are dislocation barriers inside the shear zone. Dislocation barriers are subdivided into two types: i) Kear-Wilksdorf barriers formed due to thermoactivating selfblock of screw dislocations and ii) the barriers formed due to thermoactivating blocking of edge superdislocations when the trapping of point defects on them. The temperature increase of deformation causes the accumulation intensity increase of dislocation barriers [3, 4] that results in the moving dislocations density decrease. Therein superdislocations mobility not included in barriers configuration increase. All mentioned above conditions are taken into account in the first equation in the system (1) that gives the creep rate occurring through thermoactivating dislocations movement (2):

$$\frac{da}{dt} = \rho_s^* b v_D (\xi \rho)^{-1/2} \times \left(\exp \left[-\frac{U - \tau_s b^2 l_{cp}}{kT} \right] + \exp \left[-\frac{U + \tau_s b^2 l_{cp}}{kT} \right] \right). \quad (2)$$

where b is the modulus of the Burgers vector, v_D is the Debye frequency, ξ is the fraction of forest dislocations, ρ is the dislocations density, U is the activation energy of dislocations thermo fluctuation movement along a slip plane, τ_s is the thermo activating fraction of deforming slip stress, $l_{aver} = l(1 - 0.7 \exp(-U_1/kT))$ is the average length of free segment, l is the average length of free segment while Kear-Wilksdorf barriers absence, U_1 is the formation energy of Kear-Wilksdorf barriers, k is the Boltzman constant, T is the deformation temperature, $\rho_s^* = \rho[1 - 0.5(e^{-U_1/kT} + e^{-U_2/kT})]$ is the density of mobile dislocations dependent on temperature, U_2 is the formation energy of diffusion barriers.

The second equation (3) of the system (1) gives dislocations accumulation in the time of deformation period. Both the accumulation of periphery as well as intrazone dislocations and their character are considered [11-14]. The intrazone dislocations (Kear-Wilksdorf barriers and diffusion barriers) are formed both in low and high temperature areas but with different rates. Kear-Wilksdorf barriers are intensively formed and accumulated under low and moderate temperature up to 500 K [12-14], diffusion barriers are under higher temperature (due to the higher mobility of deformation point

defects). With temperature increase diffusion barriers displace Kear-Wilsdorf barriers. This is taken into account in the second equation (3) of the system (1) by means of factors C_2 , C_3 :

$$\frac{d\rho}{dt} = \dot{\alpha} \left(C_1 \frac{(\alpha G b)^2 \rho}{\tau_f^0 + \tau_f + \alpha G b \rho^{1/2}} + \frac{C_2 e^{U_1/kT} + C_3 e^{U_2/kT}}{G b \rho^{1/2}} \right) - \min(r_s, [\theta \rho]^{-1/2}) \frac{a_l^3 D_0}{\chi k T b} \left(\exp\left[\frac{-E_i}{kT}\right] \cdot C_i + \exp\left[\frac{-E_v}{kT}\right] \cdot C_v \right) \tau \rho^2 \theta^2. \quad (3)$$

Here C_1, C_2 and C_3 are constants, $\alpha = \alpha_0 - \beta T$ is the parameter characterizing interdislocation interaction, α_0, β are constants derived from experimental dependence $\alpha(T)$, for a certain $L1_2$ alloy, G is the shear modulus, τ_f^0 is the friction stress related to overcoming of the Peierls barrier, $\tau_f = \gamma_1 \tau_0^{(1)} \exp(-U_1/kT) + \gamma_2 \tau_0^{(2)} \exp(-U_2/kT)$ is the friction stress due to the formation of Kear-Wilsdorf barriers on screw dislocations and the trapping of point defects on edge dislocations, γ_1, γ_2 is contribution factor (for uniform expanding rectangular dislocation loop $\gamma_1 = \gamma_2 = 1/2$), $\tau_0^{(1)}, \tau_0^{(2)}, \alpha_0, \beta$, are temperature independent constants, ν is Poisson's ratio, θ is the edge dislocation fraction, a_l is the lattice parameter, D_0 is the preexponential factor, χ is the orientation factor, E_i and E_v is the activation energy of interstitial atoms and vacancies, respectively; C_i и C_v is the concentrations of interstitial atoms and vacancies.

The first term of the equation (3) determines dislocations¹¹⁾ accumulation and dislocation barriers [12]; the second one determines their annihilation.

The third (4) and the forth (5) equations of the system calculate the accumulation of deformation point defects: interstitial point atoms and vacancies, respectively.

$$\frac{dC_i}{dt} = \dot{\alpha} \frac{1}{\kappa(\zeta)} p_j \xi B \frac{\tau}{G} - \frac{a_l^3 D_0}{\chi k T} \exp\left[\frac{-E_i}{kT}\right] C_i \tau \rho \theta - \mu_r D_0 \exp\left[\frac{-E_i}{kT}\right] C_i C_v, \quad (4)$$

$$\frac{dC_v}{dt} = \dot{\alpha} \frac{1}{\kappa(\zeta)} p_j \xi B \frac{\tau}{G} - \frac{a_l^3 D_0}{\chi k T} \exp\left[\frac{-E_v}{kT}\right] C_v \tau \rho \theta - \mu_r D_0 \exp\left[\frac{-E_v}{kT}\right] C_i C_v \quad (5)$$

here p_j is the fraction of forest dislocations forming jogs, $\kappa(\zeta)$ is the coefficient taking into account the fraction of jogs generating point defects, ξ is the fraction of forest dislocations, B is the constant, μ_r is the temperature-independent coefficient of own interstitial atoms and vacancies recombination [15], D_0 is the pre-exponential factor.

The equations (4), (5) presuppose the point defects to be generated (the first term) due to the non-conservative dragging of jogs by means of screw dislocations or near to it orientation [16].

Annihilation of deformation point defects in the model (1) is defined by their trapping on edge dislocations and their interdependent annihilation [17], the second and the third terms in the equations (4), (5) respectively.

The presented model in the paper gives the calculations for a number of conditions: i) tension at the constant load, ii) compression at the constant load, iii) the constant stress.

For i) and ii) conditions the different degree of plasticity deformation localization in the sample was considered. Under outer applied constant load the tension is changed because of the sample section value change during its deformation. In case of homogeneous microscopic creep the stress depends on deformation and it seems to be equal: $\tau = \tau_0(1 + \varepsilon)$ is in case of tension. $\tau = \tau_0(1 - \varepsilon)$ is in case of compression. Under microscopic deformation localization more intensive change of sample section happens and that results in stress change in the creep zone. In this case the stress is as follows: $\tau = \tau_0(1 \pm K_3 \varepsilon)$, where K_3 being the sample fraction where creep is confined.

3. Calculation results and discussion

The relation of deformation from time $\varepsilon(t)$ in case of creep of single crystal alloys with $L1_2$ superstructure is calculated according to the model (1). The parameters values needed for solving the system of equations were taken closely spaced to parameters values for Ni_3Ge alloy. The parameters values are as follows: $C_1 = 6 \cdot 10^4 \text{ N/m}^2$; $C_2 = C_{12} - T \cdot C_{12} / 1000$; $C_{12} = 5 \cdot 10^{16} \text{ N/m}^4$; $C_3 = T \cdot C_{13} / 1000$; $C_{13} = 3 \cdot 10^{22} \text{ N/m}^4$; $U_1 = 0.0094 \text{ eV}$; $U_2 = 0.72 \text{ eV}$; $\tau_0^{(1)} = 300 \text{ MPa}$; $\tau_0^{(2)} = 1700 \text{ MPa}$; $\chi = 0.48$; $\alpha_0 = 1.8$; $\beta = 1.9 \cdot 10^{-3}$; $\tau_f^0 = 50 \text{ MPa}$; $G = 8 \cdot 10^{10} \text{ N/m}^2$; $b = 2.5 \cdot 10^{-10} \text{ m}$; $a_l = \tau_f^0 \cdot 2.5 \cdot 10^{-10} \text{ m}$; $D_0 = 7.7 \cdot 10^{-5} \text{ m}^2/\text{s}$; $E_i = 0.15 \text{ eV}$; $E_v = 1.27 \text{ eV}$; $E_i^0 = 1.6 \text{ eV}$; $E_v^0 = 4.8 \text{ eV}$; $\theta = 0.5$; $\nu = 1/3$; $\Gamma = 1$; $\kappa(\zeta) = 30$; $p_j = 0.5$; $\xi = 0.5$; $B = 340$; $\mu_r = 10^{19} \text{ m}^{-2}$; $k_0 = 0.5$; $\gamma_1 = \gamma_2 = 0.5$.

The creep rate (the first equation of the system (1)) is the following:

$$\frac{d\varepsilon}{dt} = K_1 \rho_s b v_d (\xi \rho)^{-\eta_2} \exp\left[-\frac{U - K_2 \tau_s b^2 l_{cp}}{kT}\right] + K_1 \rho_s b v_d (\xi \rho)^{-\eta_2} \exp\left[-\frac{U + K_2 \tau_s b^2 l_{cp}}{kT}\right]$$

K_1 and K_2 values should be considered as adjusted parameters. Coefficient values of K_1 and K_2 used in calculation are given in the Table 1.

Table 1. Coefficient values of K_1 and K_2

$U \text{ eV}$	K_1	K_2
3.4	$1.6 \cdot 10^{-9}$	0.1
2.0	$1.0 \cdot 10^{-14}$	0.08
1.0	$1.0 \cdot 10^{-14}$	0.04

The calculation results with initial conditions

$$a(0) = 0, \rho(0) = 10^{10} \text{ m}^{-2},$$

$$C_i(0) = \exp(-E_i^0 / kT),$$

$$C_v(0) = \exp(-E_v^0 / kT), \text{ where } E_i^0 = 1.6 \text{ eV}$$

and $E_v^0 = 4.8 \text{ eV}$ is formation energy of interstitial atoms and vacancies are respectively given in Figures 1, 3, 4.

Figure 1 gives creep curves (Figure 1 *a* and *b*) and creep rate dependence on time (Figure 1 *c* and *d*) calculated in the model. Applied stresses were considered as $\tau_0 = 166.5 \text{ MPa}$ ($\sigma = 370 \text{ MPa}$) and $\tau_0 = 450 \text{ MPa}$ ($\sigma = 1000 \text{ MPa}$).

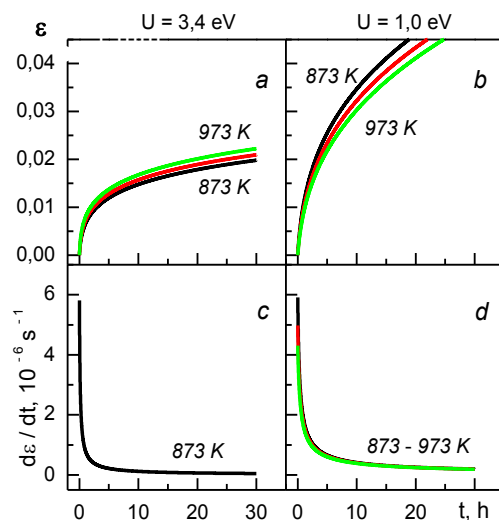


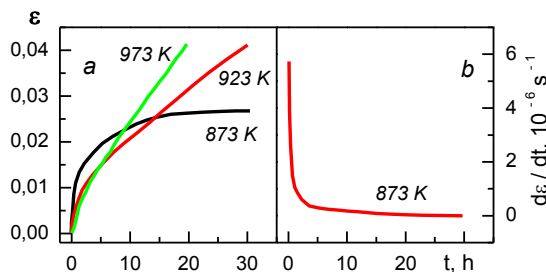
Figure 1. Calculated creep curves (*a*), (*b*) and time dependent creep rates (*c*), (*d*) for alloys with the $L1_2$ superstructure at different deformation temperatures, the activation energy of the thermoactivating superdislocation movement U , and the constant stress. Stress $\sigma = 370 \text{ MPa}$

Figure 2 gives the experimental creep curves (Figure 2 *a*) and the time dependence of creep rate (Figure 2 *b*) obtained for Ni₃Ge alloy single crystals oriented along direction [001] under its compression [18]. As well as in the experiments (Figure 2) calculated curves $\varepsilon(t)$ and $\dot{\varepsilon}(t)$ (Figure 1) demonstrate two stages of creep: the first stage is the stage of primary creep with continuous rate decrease, the second one being the stage of steady-state creep where the rate keeps stable.

The activation energy U in the range between 2.0 and 1.0 eV demonstrates anomalous creep rate dependence on temperature: temperature increase from 823 to 973 K results in creep rate decrease (Figure 1). Experimentally that situation is observed at the initial stage of the creep for Ni₃Ge alloy single crystals under the same initial load.

Load change to higher ones up to 1000 MPa (Figure 3) considerably changes the character of the creep curves due to the activation energy of the thermoactivating superdislocation movement U . During the test the linear creep with stable rate is observed in the range of activation energy U being between 1.0 to 2.0 eV. The creep anomaly characteristic to lower loads disappears in this case (Figure 3). Similar changes are observed in the experiments of Ni₃Ge alloy single crystals [18] (Figure 2.II).

I)



II)

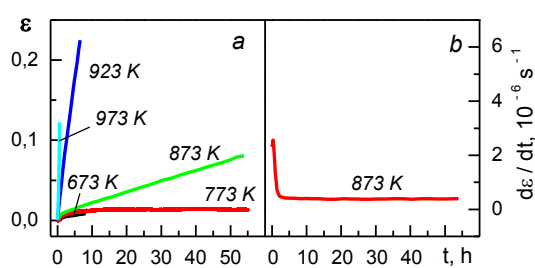


Figure 2. Experimental creep curves (*a*) and time dependent creep rates (*b*) at different deformation temperatures of the Ni₃Ge alloy single crystal [18]. The deformation axis [001]: (I) stress value $\sigma = 370$ MPa; (II) stress value $\sigma = 1000$ MPa.

The consideration of deformation localization in the creep process also shows its significant influence on creep curves (Figure 4). The influence is only quantitative in the case of compression (Figure 4 *a* and 4 *b*): without changing the character of the creep stages it results to the creep rate decrease the higher the degree of localization is.

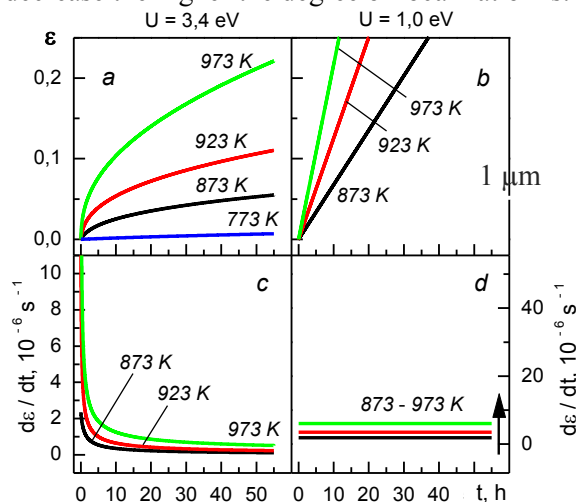


Figure 3. Calculated creep curves (*a*), (*b*) and time dependent creep rates (*c*), (*d*) for alloys with the L1₂ superstructure at different deformation temperatures, the activation energy of the thermoactivating superdislocation movement U , and the constant stress. Stress $\sigma = 1000$ MPa

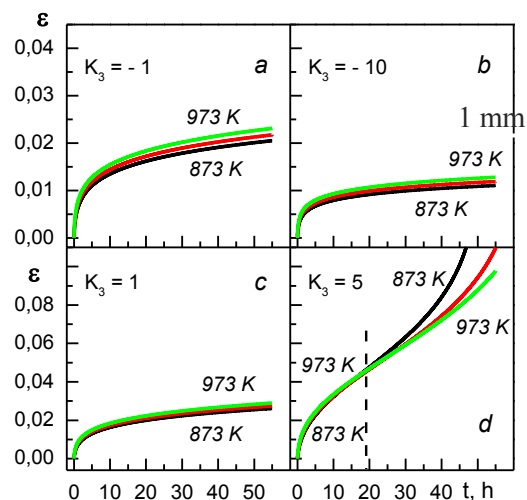


Figure 4. Calculated creep curves for alloys with the L1₂ superstructure at different deformation temperatures, the activation energy of the thermoactivating superdislocation movement $U = 3.4$ eV in case of taking into account deformation localization: (*a*), (*b*) compression, (*c*), (*d*) tension. Stress $\sigma = 1000$ MPa.

4. Conclusions

Thus, calculations testify that the creep peculiarities characteristic to $L1_2$ alloys can be defined by the model where the accumulation peculiarities and self-locking are included. Competition of the self-locking and thermoactivating superdislocation mobility leads to the creep rate anomaly in examined superstructures. The high energy of the thermoactivated superdislocation movement and low density of free and mobile superdislocations determine the low creep rate in the $L1_2$ superstructure.

Deformation localization in the creep process may cause the appearance of the inverse creep stage.

The reported study was partially supported by RFBR, research project No. 14-02-92605 KO_a.

References

- [1] Nicholls J R and Rawlings R D 1977 *J. Mater. Sci.* **12** 2456
- [2] Hemker K J and Nix W D 1989 *Mater. Res. Soc. Symp. Proc.* **133** 481
- [3] Hemker K J, Nix W D and Mills M 1991 *J. Acta Metall. Mater.* **39** 1901
- [4] Hemker K J and Nix W D 1993 *Metall. Trans. A.* **24A** 335
- [5] Rong T S, Jones I P and Smallman R E 1995 *Acta metal.* **43** 1385
- [6] W H Zhu, D Fort, I P Jones, R E Smallman 1998 *Acta mater.* **46** 3873
- [7] B H Kear, H G B Wilsdorf: Trans. Metallurg 1962 *Soc. AIME* **224** 382
- [8] Yu V Solov'eva, B I Burtsev and V A Starenchenko 2005 *Izv. Vyssh. Uchebn. Zaved., Fiz.* **9** 28 (in Russian)
- [9] Starenchenko V A, Pantyukhova O D, Solov'eva Yu V, Burtsev B I and Starenchenko S V 2005 *Phys. Met. and Metallogr.* **100** 399
- [10] Starenchenko V A, Pantyukhova O D and Starenchenko S V 2002 *Physics of the Solid State* **44** 994
- [11] Starenchenko V A, Chernykh Yu A and Abzaev Yu A 1987 *Physics of Metal* **2** 22
- [12] Starenchenko V A, Solov'eva Yu V, Abzaev Yu A 1999 *Physics of the Solid State* **41** 407
- [13] Starenchenko V A, Solov'eva Yu V, Abzaev Yu A, Kozlov E V, Shpeizman V V, Nikolaev V I and Smirnov B I 1998 *Physics of the Solid State* **40** 618
- [14] Starenchenko V A, Solov'eva Yu V, Abzaev Yu A, Nikolaev V I, Shpeizman V V and Smirnov B I 1996 *Physics of the Solid State* **38** 1668
- [15] K P Gurov, A B Tsepelev 1991 *Nuclear Materials* **182** 240
- [16] Starenchenko V A, Starenchenko S V, Kolupaeva S N and Pantyukhova O D 2000 *Russian Physics Journal* **43** 61
- [17] Starenchenko V A, Pantyukhova O D, Solov'eva Yu V 2004 *The Physic of Metals and Metallography* **97** 545
- [18] Solov'eva Yu V, Gettinger M V, Starenchenko S V and Starenchenko V A 2009 *Russian Physics Journal* **52** 390